

Formation characteristic of Ca–P coatings on magnesium alloy surface

Guang-yi LIU¹, Sha-wei TANG¹, Chuan WANG¹, Jin HU¹, De-chao LI²

1. School of Materials Science and Engineering, Harbin Institute of Technology, Harbin 150001, China;

2. School of Stomatology, Jiamusi University, Jiamusi 154002, China

Received 12 June 2012; accepted 27 November 2012

Abstract: A chemical method was used to deposit dicalcium phosphate dehydrate coatings on AZ91 magnesium alloy. The aim was to improve the biodegradation behavior of magnesium alloy in a simulated body fluid. The microstructures of the coating before and after immersion in the simulated body fluid were characterized by scanning electron microscopy (SEM) and X-ray diffraction (XRD). The results indicated that the dicalcium phosphate dehydrate coatings exhibited two morphologies during the pre-calcification process. The titration speed of the pre-calcification process had great influence on the morphologies of the pre-calcification coatings. As the soaking time increased, the diffraction peaks of dicalcium phosphate dehydrate disappeared and hydroxyapatite precipitated on the coated substrate surfaces. This indicates the dissolution of dicalcium phosphate dehydrate during the immersion process. The structures of the dicalcium phosphate dehydrate coatings and the formation mechanisms of the hydroxyapatite coatings were investigated in detail.

Key words: magnesium alloy; Ca–P coatings; microstructure; simulated body fluid

1 Introduction

As a lightweight metal with mechanical properties similar to those of natural bone, Mg and its alloys are potential biodegradable materials and are widely used as biocompatible, degradable implants for load-bearing applications [1–3]. However, Mg exhibits poor corrosion properties, which results in the loss of mechanical integrity before tissue healing. Surface modification of Mg alloys is regarded as an effective method to improve their corrosion resistance. Calcium phosphate coatings improve the biocompatibility of metallic implants and increase bone growth at the site of implantation [4–6]. In particular, biomimetically deposited coatings are receiving more and more attention because of their excellent biocompatibility [7,8].

SONG et al [9] obtained hydroxyapatite (HA) on an Mg alloy by electrodeposition method to improve the biodegradation behavior of Mg alloy in a human body environment. They found that the as-deposited coatings consisted of dicalcium phosphate dehydrate (DCPD) and β -tricalcium phosphate (β -TCP), which was transformed to HA after immersion in NaOH solution, indicating that

DCPD and β -TCP are the precursors of HA. Earlier work [10] reported the DCPD deposition on pure magnesium by putting the samples into a mixed solution involving Na_2HPO_4 and $\text{Ca}(\text{NO}_3)_2$. But they reported that no HA phases formed on the DCPD-coated samples after being soaked in SBF. Our previous study [11] indicated that DCPD coatings were deposited on the surface of AZ91, and that DCPD not only transformed into HA but also induced HA precipitation after being immersed in SBF, resulting in the corrosion resistance increasing with the increase of soaking time.

DCPD is the precursor of HA [7,12]. It could be dissolved in a physiological environment, and HA precipitation occurs after being soaked in simulated body fluid (SBF). In fact, the formation of biomimetic apatite is highly dependent on the structure and composition of the substrate [13,14]. In this work, a pre-calcification treatment is performed on the surface of AZ91 alloy to form a surface structure favorable to the apatite deposition. Subsequently, an HA-like coating is generated on the pre-calcified substrate in a SBF. The structures and morphologies of the pre-calcified coatings are investigated and the formation mechanism of HA on the pre-calcified substrate in the SBF is also explored.

2 Experimental

The substrate was AZ91 magnesium alloy. The specimen ($d15\text{ mm} \times 3\text{ mm}$) surfaces were ground with 1500 grit SiC paper to ensure the same surface state and ultrasonically cleaned in ethanol, then air dried. The specimens were put into 0.17 mol/L $\text{Ca}(\text{NO}_3)_2$ solution (500 mL), followed by 0.10 mol/L K_2HPO_4 solution (500 mL) immediately being dribbled into the solution. In the beginning, 250 mL of K_2HPO_4 was dribbled into the $\text{Ca}(\text{NO}_3)_2$ solution at a speed of 5 mL/min, and then the residual 250 mL of K_2HPO_4 was dribbled into the $\text{Ca}(\text{NO}_3)_2$ solution at a speed of 1 mL/min. With the addition of K_2HPO_4 , calcium phosphate phases began to precipitate. Subsequently, the samples were kept staying in the mixed solution for 3 h. A pre-calcified coating was obtained on the substrate surfaces. The bone-like calcium phosphate layer was prepared by immersing the pre-calcified samples in a SBF solution at 37 °C for different times. The solution pH was adjusted to 7.4. The composition of the SBF was the same as that of Ref. [15]. The SBF was refreshed every 24 h. After soaking, the samples were removed from the SBF, rinsed with distilled water and dried at room temperature.

Auxiliary techniques such as scanning electron microscopy (SEM, Hitachi S-3000N), X-ray diffraction (XRD, Philips X'Pert diffractometer) and Fourier transform infrared spectroscopy (FT-IR) and inductively coupled plasma optical emission spectroscopy (ICP-OES) analyses were used.

The electrochemical behaviour of the pre-calcified samples was investigated by open circuit potential (OCP) evolution using a 273A potentiostat with a three-electrode cell configuration.

3 Results

3.1 Morphologies of coatings

The typical SEM micrographs of the pre-calcification coatings are shown in Fig. 1. The coatings exhibit a special nano-micro two-level structure, i.e., feather-shaped and plate-like structure (Fig. 1(a)). At higher magnification, it can be seen that the feather-shaped crystals formed on the substrate exhibit a nanoflake structure, as shown in Fig. 1(b). Moreover, from Fig. 1, it can be seen that the surfaces of these crystals (either plate-like or feather-shaped) are rather smooth.

Figure 2 shows the evolution of surface morphologies of the coatings growing on the pre-calcified surfaces during the SBF incubation process. After 5 h of immersion in the SBF, a majority of the plate-like crystal characteristics disappear, while the

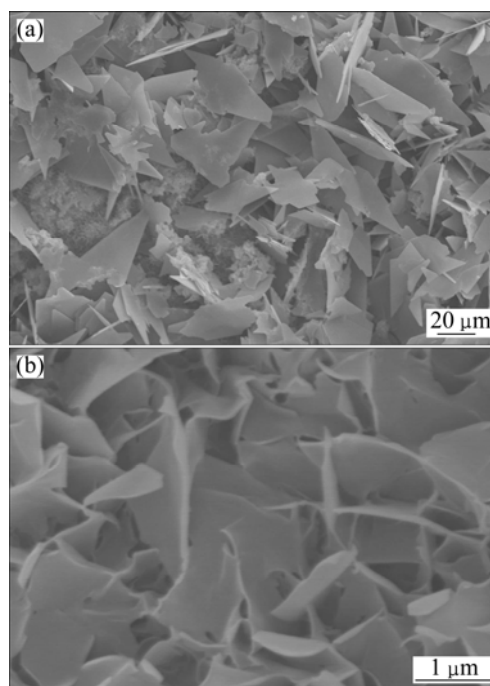


Fig. 1 Morphologies of DCPD coating: (a) Low magnification; (b) High magnification

original feather-like DCPD crystals are still present on the substrate surface, which exhibits a nanoflake structure. As the immersion time increases, the surface morphologies of the coatings change gradually. Flake-shaped crystals, rod-like particles and spherical precipitate can be observed on the coating surface clearly. Moreover, it is found that many small particles are deposited on the surfaces of these crystals. Compared with the surface of crystals shown in Fig. 1, these crystals exhibit a rough surface composed of a large number of networks (Figs. 2(b), (c) and (d)), which indicates that nano-crystal precipitates appear on the pre-calcified surface.

3.2 Structure of pre-calcified coatings before and after soaking in SBF

Figure 3 displays the XRD patterns of the pre-calcified samples measured under the grazing incidence condition. The surface composition of the pre-calcified samples at different soaking time is presented. The XRD results reveal that the pre-calcification phases on the substrate are mainly DCPD. Magnesium peaks are also detected by the XRD analysis.

After immersing the pre-calcified sample in the SBF for 1 h, the diffraction peaks of DCPD are still present on the substrate surface, but have a significantly lower intensity than that on the pre-calcified surface, suggesting the dissolution of the DCPD coatings. The diffraction peaks of DCPD disappear completely after 5 h of immersion, but new diffraction peaks appear in the

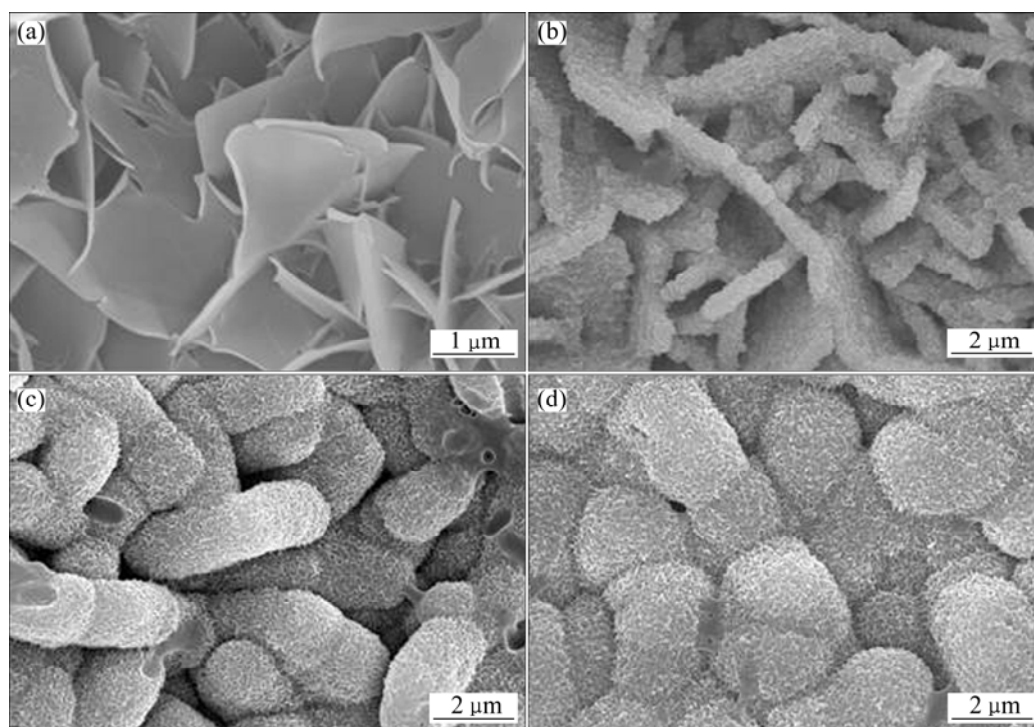


Fig. 2 Surface morphologies of DCPE-coated samples after immersion in SBF for different time: (a) 5 h; (b) 24 h; (c) 48 h; (d) 120 h

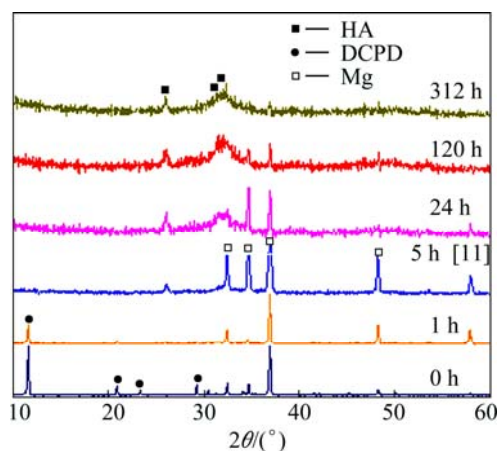


Fig. 3 XRD patterns of pre-calcified samples after immersion in SBF for different time

XRD pattern [11]. Apatite reflections are obtained. It implies that, after being soaked in SBF for a short time, the main phases in the pre-calcified coatings evolve from DCPD toward an apatite phase. As the immersion time increases, more HA diffraction peaks are observed in the XRD patterns. The relative intensity of the HA peaks is significantly high and the intensity of Mg peaks reduce remarkably after being soaked in the SBF for 312 h, which reveals that more HA present on the substrate surface.

The results of XRD indicate that not only the DCPD coating on the substrate surface is transformed into HA, but also a new HA coating continuously precipitates on

the pre-calcified surface with the increasing of soaking time, resulting in the thickness increasing of the coatings on the substrate surface.

FT-IR spectroscopy was used to examine the chemical structure of the DCPD coatings after being soaked in the SBF for 24 and 120 h. The FT-IR spectra (Fig. 4) indicate that the chemical structure of the coatings has no changes after being soaked in the SBF for more than 24 h. As can be seen in Fig. 4, broad absorption band at 3440 cm^{-1} and bending mode at 1650 cm^{-1} are attributed to H_2O in the DCPD coatings after SBF incubation. The vibrational bands at 563, 604 and 1030 cm^{-1} can be confirmed as the typical peak of PO_4^{3-} . The spectra clearly illustrate two sharp absorption

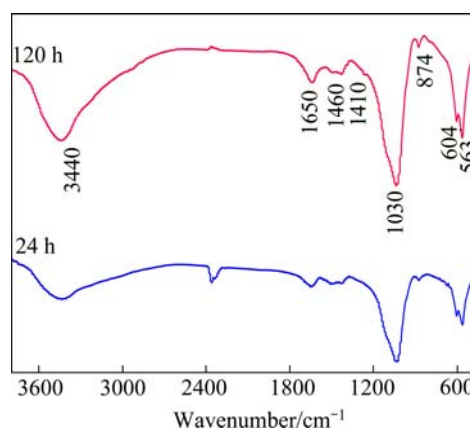


Fig. 4 FT-IR spectra of pre-calcified sample soaked in SBF for different time

bands of $\nu_3 \text{PO}_4$ at 563 and 604 cm^{-1} , ascribing to crystalline calcium phosphate. It indicates that DCPD in the coatings tends to convert to apatite after being soaked in the SBF, which affirmed the XRD results.

The ionic concentrations of the SBF with the immersion of DCPD-coated sample were measured as a function of the immersion time, as shown in Fig. 5. As can be seen in Fig. 5, in the first 5 h immersion, the Ca and P concentrations of the SBF solution increase, indicating that Ca and P are released from the pre-calcification coatings into the SBF solution. It can be affirmed that the increase in Ca and P concentrations is mainly due to the dissolving of the DCPD phases in the SBF, consistent with our previous study [11]. Nevertheless, the Ca and P concentrations of the SBF solution began to decrease after 12 h of SBF immersion. This is due to the nucleation and growth of the apatite consuming Ca and P in the SBF solution, thus, the amount of Ca and P in the SBF reduces. Na concentration of the SBF does not change obviously, in addition, no obvious dissolution of Mg in the substrate is observed.

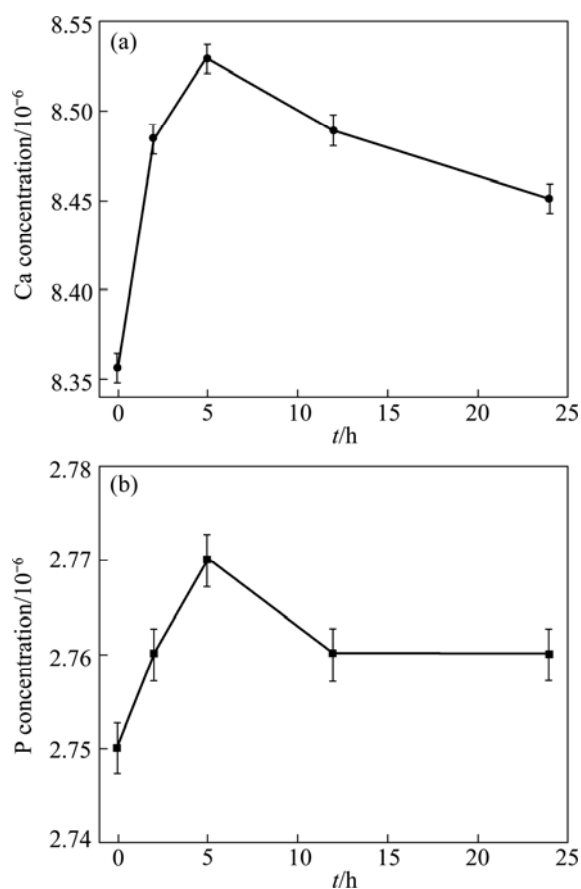


Fig. 5 Change in Ca (a) and P (b) concentrations of SBF during SBF immersion process

3.3 Electrochemical behavior

Figure 6 shows the open circuit potential (OCP) as a function of time for the pre-calcified substrate exposed to

the SBF for 70 ks. At first, the OCP increases rapidly, but drops quickly thereafter. Subsequently, the OCP rises gradually as the coating develops over the pre-calcified surface.

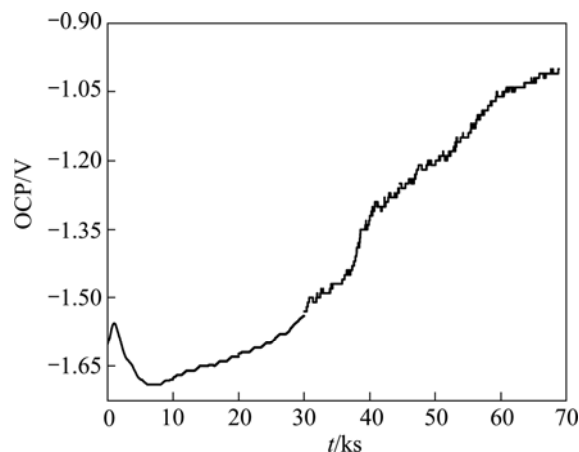


Fig. 6 Open circuit potential evolution of pre-calcified sample immersed in SBF solution as function of exposure time

The potential increases in the initial stage of immersion. It may be a rapid precipitation of calcium phosphate crystals from solution, since the solutions are unstable. According to the above analysis, one can conclude that the dissolution of DCPD is proceeding over the succedent time of immersion which can be confirmed by measurement of the concentration of Ca and P in SBF, as shown in Fig. 5 and a decrease in OCP is shown in this period. Subsequently, the OCP shows an increase, indicating that the DCPD dissolution promotes the nucleation of HA. In this case, the formation and growth of the HA precipitates along with the transformation of DCPD take place during the immersion process, until the whole pre-calcified surface is covered by formed coatings, accordingly resulting in the potential increasing.

4 Discussion

4.1 Preparation and structure of DCPD coating

When the fresh magnesium alloy surface is exposed to the pre-calcified solution ($\text{Ca}(\text{NO}_3)_2$ solution), gas bubbles rise from the sample surface due to the corrosion of Mg in the acidic solution through the following reactions [10]:



The dissolution of Mg on the substrate surface is considered to provide favorable sites for DCPD nucleation due to the significant alkalization near the surface (Eq. (2)). During the pre-calcification process, Ca^{2+} reacts with HPO_4^{2-} to form DCPD.



With the increase of K_2HPO_4 , lots of DCPD nuclei are formed on the substrate surface and then DCPD grows spontaneously by consuming the Ca^{2+} and HPO_4^{2-} from the surrounding fluid.

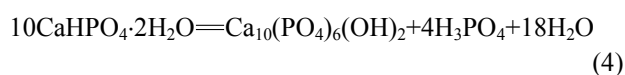
The two morphologies appearing in the pre-calcified coating imply that the titration speed of the pre-calcification process has an intense influence on the morphology of the pre-calcification coatings. In the initial stage of pre-calcification, the K_2HPO_4 is titrated quickly in $\text{Ca}(\text{NO}_3)_2$ solution. As a result of the speediness of the titration, the DCPD nucleates quickly on the substrate surface as soon as the samples are soaked in $\text{Ca}(\text{NO}_3)_2$ solution and accordingly plate-like crystals form on the substrate surface. Some active regions on the substrate surface are firstly covered by the plate-like crystals along with the corrosion of substrate owing to Mg being corroded easily in an acid solution. Subsequently, the residual K_2HPO_4 is titrated slowly into the $\text{Ca}(\text{NO}_3)_2$ solution. In this case, the reaction of Ca^{2+} with HPO_4^{2-} to form DCPD occurs on the substrate surface every where. Thus feather-like crystals could be observed on the substrate surface. Moreover, the formed pre-calcification coatings have enough time to grow, and plate-like crystals also appear on the substrate surface during the slow titration process.

4.2 Mechanism for formation of apatite

DCPD is the precursors of HA. HA is the best stable calcium phosphate ceramic in alkaline solution. The dissolution of DCPD in the SBF promotes the nucleation of HA.

LU and LENG [12] analyzed the free energy change of Ca–P precipitation (ΔG) and the Ca–P nucleation rate (J) in SBF. They found that the HA precipitates are thermodynamically favorable when $\text{pH} > 5.4$, because ΔG_{HA} becomes negative. However, there is no thermodynamic driving force for the DCPD precipitation ($\Delta G_{\text{DCPD}} > 0$) over the entire pH range. The analysis indicates that HA precipitates exhibit a higher thermodynamic driving force than octacalcium phosphate (OCP) and DCPD in SBF. The HA nucleation rate is significantly affected by the pH value. A high pH environment is favorable for HA nucleation.

DCPD is transformed into HA after being soaked in SBF. The following reaction shows the transforming process:



During the immersion process, HA would be formed (as shown in Figs. 1 and 3). The dissolution of DCPD coatings on the pre-calcified surface of Mg alloy is considered to provide favorable sites for HA

nucleation. With increasing in soaking time, the HA nucleation is accelerated by increasing the supersaturation of the solution with respect to HA [13]. Consequently, lots of HA nuclei are formed on the substrate surface and then HA would grow spontaneously by consuming the calcium and phosphate ions from the surrounding fluid [14].

The protection capacity of the substrate not only depends on the chemical nature of the coating itself, but also has great relation with the stability of the coating. The feather-like morphology of DCPD coatings would offer a much larger surface to contact with the SBF solution and induce more apatite to deposit. From the results of the electrochemical corrosion testing analysis, the preparation of the coating with high stability would prevent Mg alloy substrate from rapidly corroding in the SBF.

From Fig. 2, it can be clearly found that the HA coating is not compact and displays uniform network-like morphologies. The loose HA coatings are helpful for the bone tissue to infiltrate into the implants then to accelerate the healing of the damaged bone [15].

5 Conclusions

The precursor of dicalcium phosphate dehydrate coating was obtained on AZ91 magnesium alloy by a chemical method to improve the biodegradation behaviors of magnesium alloy in the simulated body fluid. The titration speed of the pre-calcification process has great influence on the morphologies of the pre-calcification coatings. The dicalcium phosphate dehydrate coating exhibits two morphologies during the pre-calcification process, which is attributed to the different titration rate of the coating process. The precipitation layer of hydroxyapatite coatings shows a rough and porous surface structure which contains numerous nano-networks. The precipitate of hydroxyapatite coatings on the pre-calcified surface after being soaking in the simulated body fluid provides a good protection for the substrate.

References

- [1] STAIGER M P, PIETAK A M, HUADMAI J, DIAS G. Magnesium and its alloys as orthopedic biomaterials: A review [J]. *Biomaterials*, 2006, 27: 1728–1734.
- [2] ZHANG Jia, ZONG Yang, YUAN Guang-yin, CHANG Jian-wei, FU Peng-huai, DING Wen-jiang. Degradable behavior of new-type medical Mg–Nd–Zn–Zr magnesium alloy in simulated body fluid [J]. *The Chinese Journal of Nonferrous Metals*, 2010, 20(10): 1990–1997. (in Chinese)
- [3] ZENG Rong-cang, KONG Ling-hong, CHEN Jun, CUI Hong-zhi, LIU Cheng-long. Research progress on surface modification of magnesium alloys for medical applications [J]. *The Chinese Journal of Nonferrous Metals*, 2011, 21(1): 35–43. (in Chinese)

- [4] PULEO D A, NANJI A. Understanding and controlling the bone-implant interface [J]. *Biomaterials*, 1999, 20: 2311–2321.
- [5] ZHANG Chun-yan. The study on preparation and biodegradation behavior of bioceramic coatings on magnesium alloy [D]. Chongqing: Chongqing University, 2011: 2–4. (in Chinese)
- [6] GAO Jia-cheng, LI Long-chuan, WANG Yong. Surface modification on magnesium by alkali-heat-treatment and its corrosion behaviors in SBF [J]. *The Chinese Journal of Nonferrous Metals*, 2004, 14(9): 1508–1513. (in Chinese)
- [7] ZHANG E, YANG K. Biomimetic coating of calcium phosphate on biometallic materials [J]. *Transactions of Nonferrous Metals Society of China*, 2005, 15: 1199–1205.
- [8] ZHANG Q, LENG Y. Electrochemical activation of titanium for biomimetic coating of calcium phosphate [J]. *Biomaterial*, 2005, 26: 3853–3859.
- [9] SONG Y W, SHAN D Y, HAN E H. Electrodeposition of hydroxyapatite coating on AZ91D magnesium alloy for biomaterials application [J]. *Materials Letters*, 2008, 62: 3276–3279.
- [10] WANG Y, WEI M, GAO J C. Improve corrosion resistance of magnesium in simulated body fluid by dicalcium phosphate dehydrate coating [J]. *Materials Science and Engineering C*, 2009, 29: 1311–1316.
- [11] HU J, WANG C, REN W C, ZHANG S, LIU F. Microstructure evolution and corrosion mechanism of dicalcium phosphate dihydrate coating on magnesium alloy in simulated body fluid [J]. *Materials Chemistry Physics*, 2010, 119: 294–298.
- [12] LU X, LENG Y. Theoretical analysis of calcium phosphate precipitation in simulated body fluid [J]. *Biomaterials*, 2005, 26: 1097–1108.
- [13] JONASOVA L, MULLER F A, HELEBRANT A, STRNAD J, GREIL P. Biomimetic apatite formation on chemically treated titanium [J]. *Biomaterials*, 2004, 25: 1187–1194.
- [14] KOKUBO T. Formation of biologically active bone-like apatite on metals and polymers by a biomimetic process [J]. *Thermochimica Acta*, 1996, 280–281: 479–490.
- [15] KOKUBO T, TAKADAMA H. How useful is SBF in predicting in vivo bone bioactivity [J]. *Biomaterials*, 2006, 27: 2907–2915.

Ca-P 涂层在镁合金表面的形成特征

刘广义¹, 唐莎巍¹, 王川¹, 胡津¹, 李德超²

1. 哈尔滨工业大学 材料科学与工程学院, 哈尔滨 150001;

2. 佳木斯大学 口腔医学院, 佳木斯 154002

摘要: 用化学方法在 AZ91 镁合金表面沉积二水磷酸氢钙涂层以提高镁合金在模拟体液中的生物降解能力。运用扫描电镜、X 射线衍射对该涂层在模拟体液中浸泡前、后的显微组织进行分析。结果表明, 在预钙化过程中形成的二水磷酸氢钙涂层呈现出两种不同的形貌。预钙化过程中钙化溶液的滴定速度强烈地影响预钙化涂层的形貌。随着钙化涂层在模拟体液中浸泡时间的延长, 二水磷酸氢钙的衍射峰逐渐消失, 羟基磷灰石在基底表面析出, 表明二水磷酸氢钙在浸泡过程中发生溶解。详细讨论了二水磷酸氢钙涂层的结构以及羟基磷灰石涂层的形成机制。

关键词: 镁合金; Ca-P 涂层; 显微组织; 模拟体液

(Edited by Sai-qian YUAN)